The impact of SST on the wind and air temperature simulations: a case study for the coastal region of the Rio de Janeiro state

Ian C. D. V. Dragaud, Mauricio Soares da Silva, Luiz Paulo F. Assad, Márcio Cataldi, Luiz Landau, Renato N. Elias, Luiz Claudio G. Pimentel, Jimy Dudhia

1. Introduction

NWP models are important tools capable of representing the diurnal variations of the wind field related with land-sea breezes and variations induced by SST gradients. Nowadays, many gap-free Sea Surface Temperature (SST) products are available for the scientific community, each with its own characteristics. These products are generated by methodologies that combine satellites measurements and in situ data. Over the Brazilian Southeast continental shelf, in the vicinity of state of Rio de Janeiro, strong SST gradients occur associated with the coastal upwelling (Franchito et al. 2008). The localization and magnitude of these gradients are variable among SST products (Castelão 2012), impacting the NWPs. In order to obtain a better numerical representation of the coastal region of the state of Rio de Janeiro, this study investigates the use of two SST products for the initial and boundary conditions to the Weather Research and Forecasting (WRF) model and its impacts on air temperature and near-surface atmospheric flow.

2. Data and methods

2.1 Period

The study period comprised January 24 to 26, 2014, characterized by the continuous occurrence of coastal upwelling (SST < 18 °C) in the Central and East Coast and dominance of the South Atlantic Subtropical Anticyclone (SASA) over the state.

2.2 WRF Model and experiments

The simulations are performed with the Weather Research and Forecasting model (WRF, Skamarock et al. 2008) version 3.6. The model is configured with a total of three domains applying a telescopic one-way nesting (Fig. 1b). All the three nested domains were configured with the same stretched vertical grid with 35 levels, including seven levels below 1 km. Physical parameterizations include the Rapid Radiative Transfer Model longwave radiation (Mlawer et al. 1997), the Dudhia shortwave radiation scheme (Dudhia 1989), the WRF single-moment 3-class microphysics scheme (Hong et al. 2004), the Betts-Miller-Janjic cumulus parameterization scheme (Janjic 1994), the Noah-MP land surface model (Niu et al. 2011), the Revised MM5 Monin-Obuckov (Jimenez et al. 2012) for surface layer, and the Grenier-Bretherton-McCaa Planetary Boundary Layer scheme (Grenier and Bretherton 2001).

Initial and lateral boundary conditions from Global Forecast System (GFS) forecast results were provided to the WRF model. The GFS forecast results have three-hour intervals, a horizontal resolution of 0.5°x0.5° and came from the simulation initialized at 00 UTC 24 January 2014. Two sets of numerical simulations were performed using the WRF model. The first experiment, called EGFS, used the GFS forecast results to prescribe the initial and boundary conditions. In the second, called EMUR, The SST was replaced by the Multi-scale Ultra-high Resolution Sea Surface Temperature (MUR SST). The SST boundary condition was updated daily in both experiments.

2.3 SST products

The GFS SST initial and boundary condition are composed by the weekly 1° (~111 km) spatial resolution optimum interpolation SST analysis (Reynolds et al. 2002). The MUR SST analysis is a daily product, globally gridded at approximately 1 km resolution. More information can be found at http://mur.jpl.nasa.gov/.

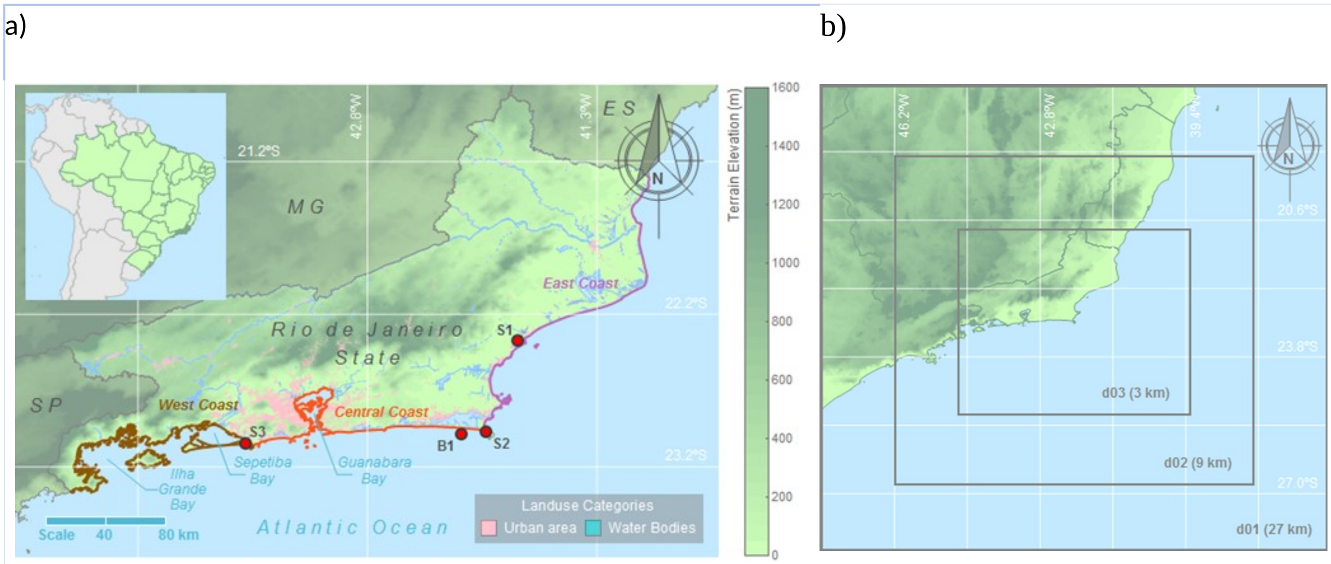

Fig. 1 a) State area and location in Brazil. S1, S2 and S3 indicate the surface weather observation stations sites of Macaé, Arraial do Cabo and Marambaia, respectively, and B1 indicates the buoy site. The elevation and the land use categories of the urban area and water bodies are also shown. The coastline was divided into West, Central and East Coasts to facilitate the following analyses. b) The three nested model domains used in WRF. The elevation is also shown

2.4 Analyses

Results from both experiments using the high-resolution grid (3 km) will be presented. The first 6 hours are discarded as a spin-up. The wind direction differences between the experiments were calculated following Jiménez and Dudhia (2013). The results from the grid points on land that are nearest to the surface weather observation stations sites are compared with the observations taken over this sites. Similarly, the results from the grid point on the water that is nearest to the buoy site are compared with the buoy data.

3 Results and Discussion

3.1 SST fields

The bigger differences between the EGFS SST and the EMUR SST occurs close to the coast (Fig. 2c), which highlights the importance of assessing the SST products for coastal regions. While in the East and Central Coasts there are intense gradient and lower SST values in the EMUR (22 °C) related to the upwelling (Fig. 2b), in the EGFS there are a weak gradient and higher SST values (26 °C) (Fig. 2a). On the West Coast, the pattern is inverse, strong gradient and the lowest SST values are in the EGFS, with differences of up to 10 °C between the experiments (Fig. 2c).

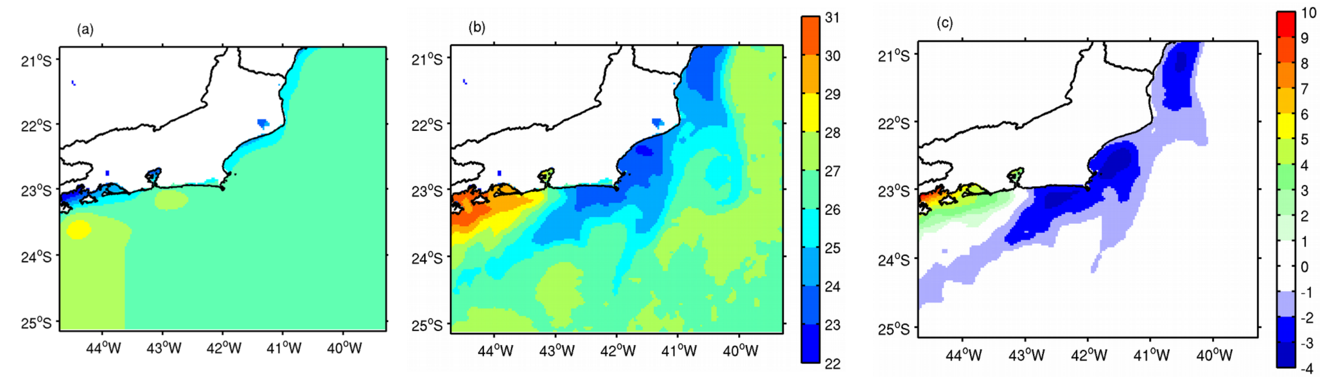

Fig. 2 SST fields (°C) on 25 January 2014: a EGFS, b EMUR, c difference between the experiments [EMUR-EGFS]

3.2 Meteorological fields

Over the ocean, the T2m (Fig. 3a,b) primarily responded to SST, following the same spatial pattern of the SST fields (Fig. 2). Over the land surface, the difference of T2m between the two experiments was not as intense as over the ocean.

In the East Coast and the eastern portion of the Central Coast, where the EMUR showed the lowest SST values related to the upwelling, the wind was weaker in the EMUR as compared to that in the EGFS (Fig 3c,d). In the West Coast and the western portion of the Central Coast, where the EMUR SST was higher, the wind was stronger compared to the EGFS. The model was not too sensitive to the land-sea gradient variation near the coastline in large part of the coast (Fig 3c,d). Since at 18 UTC the T2m increase over the continent occurred in both experiments, the lower EMUR SST in the East Coast led to a greater land-sea thermal gradient, which should increase the wind intensity, in comparison to the EGFS. Likewise, the EMUR should represent weaker winds than the EGFS in the West Coast, due to the higher SST which resulted in a lower land-sea thermal gradient at 18 UTC. Exclusively on the West Coast, the numerical experiments showed significant wind direction differences, higher than 90°, where SST differences of up to 10 °C are verified (Fig 3e,f).

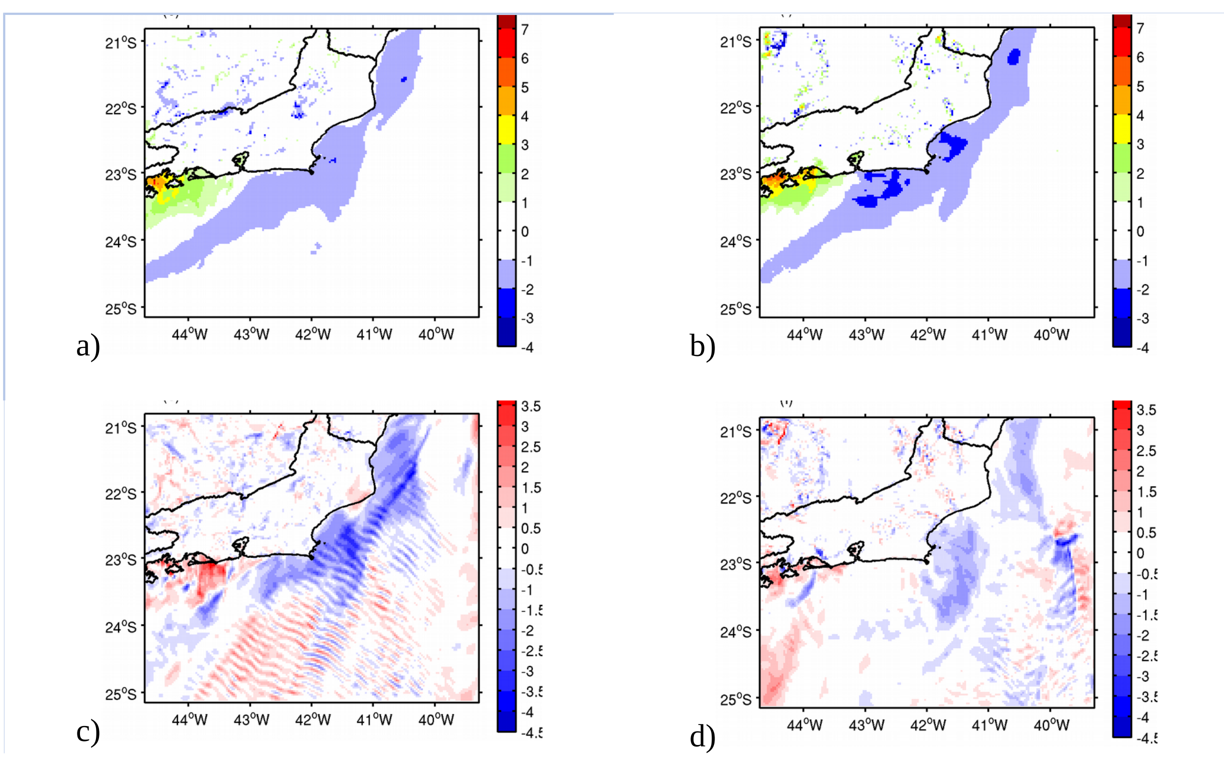

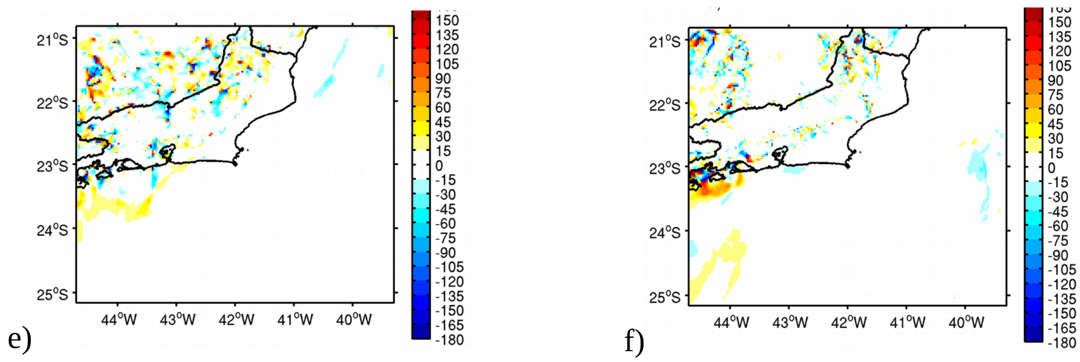

Fig. 3 Difference between the experiments [EMUR - EGFS] on 25 January 2014 at 06 UTC (left) and at 18 UTC (right). T2m AGL fields (°C): a, b. Wind speed at 10 m (ms-1): c, d. wind direction: e, f

References

Castelão RM (2012) Sea surface temperature and wind stress curl variability near a cape. J Phys Oceanogr 42:2073-2087

Dudhia J (1989) Numerical study of convection observed during the winter monsoon experiment using a mesoscale two-dimensional model. J Atmos Sci 46:3077-3107

Franchito SH, Oda TO, Rao VB, KAYANO MT (2008) Interaction between coastal upwelling and local winds at Cabo Frio, Brazil: an observational study. J appl Met Climatol 47:1590-1598.

Grenier H, CHRISTOPHER SB (2001) A moist PBL parameterization for large–scale models and its application to subtropical cloud–topped marine boundary layers. Mon Wea Rev 129:357-377

Hong S-Y, Dudhia J, Chen S-H (2004) A revised approach to ice microphysical processes for the bulk parameterization of clouds and precipitation. Mon Wea Rev 132:103-120

Janjic ZI (1994) The step-mountain eta coordinate model: further developments of the convection, viscous sublayer and turbulence closure schemes. Mon Wea Rev 122:927-945

Jiménez PA, Dudhia J, González-Rouco JF, Navarro J, Montávez JP, García-Bustamante E (2012) A revised scheme for the WRF surface layer formulation. Mon Wea Rev 140:898-918

Jiménez PA, Dudhia J (2013) On the ability of the WRF model to reproduce the surface wind direction over complex terrain. J Appl Meteor Climatol 52:1610-1617

Mlawer EJ, Taubman SJ, Brown PD, Iacono MJ, Clough SA (1997) Radiative transfer for inhomogeneous atmosphere: RRTM, a validated correlated-k model for the longwave. J Geophys Res 102:16663-16682

Niu G-Y, Yang Z-L, Mitchell KE, Chen F, Ek MB, Barlage M, Kumar A, Manning K, Niyogi D, Rosero E, Tewari M, Xia Y (2011) The community Noah land surface model with multiparameterization options (Noah - MP): 1. Model description and evaluation with local-scale measurements. J Geophys Res 116:D12109

Reynolds RW, Rayner NA, Smith TM, Stokes DC, Wang W (2002) An improved in situ and satellite SST analysis for climate. J Climate 15:1609-1625

Skamarock WC, Klemp JB, Dudhia J, Gill DO, Barker DM, Duda M, Huang XY, Wang W, Powers JG (2008) A description of the advanced research WRF version 3. Tech. Rep. TN-475+STR, NCAR